Proceedings of "Applications of Physics in Mechanical and Material Engineering" (APMME 2024)

The Influence of the Filling Factor on the Formation of Local Resonance Regions in a Two-Dimensional Phononic Hexagonal Structure

S. Garus* and A. Jurczyńska

Department of Mechanics and Fundamentals of Machinery Design, Faculty of Mechanical Engineering, Czestochowa University of Technology, Dąbrowskiego 73, 42-201 Częstochowa, Poland

Doi: 10.12693/APhysPolA.147.172 *e-mail: sebastian.garus@pcz.pl

The paper presents the influence of the fill factor of the elementary cell of a quasi-two-dimensional phononic structure with a hexagonal arrangement. The propagation of a mechanical wave in the structure was studied in the range of selected acoustic frequencies using the finite difference algorithm in the time domain. As a result of multiple reflections of the mechanical wave, as well as the occurring diffraction and interference phenomena, local resonance areas are created inside the structure, which have a significant impact on the occurrence of the phononic band gap phenomenon, i.e., such frequency bands for which the wave does not propagate in the structure. In addition, local resonance areas reduce the transmission speed of the mechanical wave front in the phononic structure.

topics: finite difference time domain algorithm (FDTD), local resonant regions, acoustic barriers

1. Introduction

The periodic distribution of the material in space causes the mechanical wave propagating in the composite to undergo diffraction and interference. Due to multiple reflections inside the phononic crystal, mechanical waves of specific frequencies penetrate the structure only partially and then are reflected. Depending on the geometry of the meta-atoms and their distribution, waves of selected frequencies do not propagate through the structure, and this phenomenon is called the occurrence of a phononic band gap.

Numerous numerical algorithms can be used to analyze the properties of phononic structures, such as the eigenmodes matching theory [1], unfitted Nitsche's method [2], the boundary integral equation method [3], the plane wave expansion method [4–6], one-dimensional transmission line model [7], the finite element method [8–10], multiple scattering theory [11, 12], the plane wave finite element method [13], the transmission matrix method [14–17], the boundary element method [18, 19], local radial basis function collocation method without mesh [20, 21]. In this paper, the finite difference time domain algorithm (FDTD) [22–24] was used to analyze wave propagation.

In this work, the mechanical wave propagation in a quasi-two-dimensional phononic structure with hexagonally arranged meta-atoms for different filling factors was analyzed.

2. Research

The pressure changes p and the instantaneous particle velocities $\boldsymbol{v}$ in materials with density ρ and acoustic impedance Z are related to each other by

$$\frac{\partial p}{\partial t} = -Z\, c\, \nabla \cdot \boldsymbol{v}, \tag{1}$$

$$\frac{\partial \boldsymbol{v}}{\partial t} = -\frac{1}{\rho}\, \nabla p. \tag{2}$$

Using the gradient of function $\boldsymbol{F}$ in the form $\nabla \boldsymbol{F} = (\partial F/\partial x_1, \partial F/\partial x_2, \ldots, \partial F/\partial x_n)$ and the divergence as $\nabla \cdot \boldsymbol{F} = (\partial/\partial x, \partial/\partial y, \partial/\partial z) \cdot (F_x, F_y, F_z) = \partial F_x/\partial x + \partial F_y/\partial y + \partial F_z/\partial z$ and expanding (1) and (2) to the two-dimensional case in Cartesian space, we obtain

$$\frac{\partial p}{\partial t} = -Z\, c \left(\frac{\partial v_x}{\partial x} + \frac{\partial v_y}{\partial y} \right), \tag{3}$$

$$\frac{\partial v_x}{\partial t} = -\frac{1}{\rho} \frac{\partial p}{\partial x}, \tag{4}$$

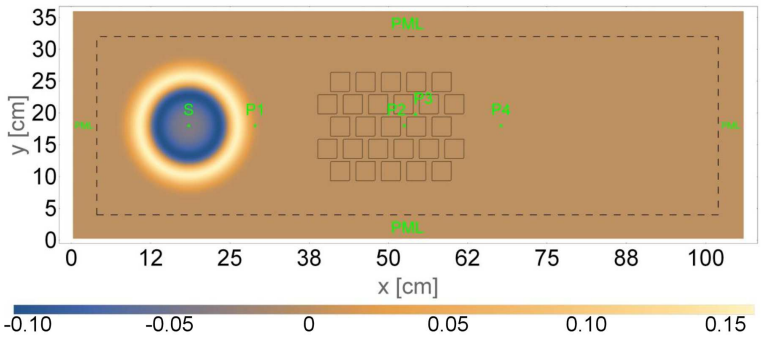

Fig. 1. Computational area for the structure with $f = 65\%$ after 700 time steps.

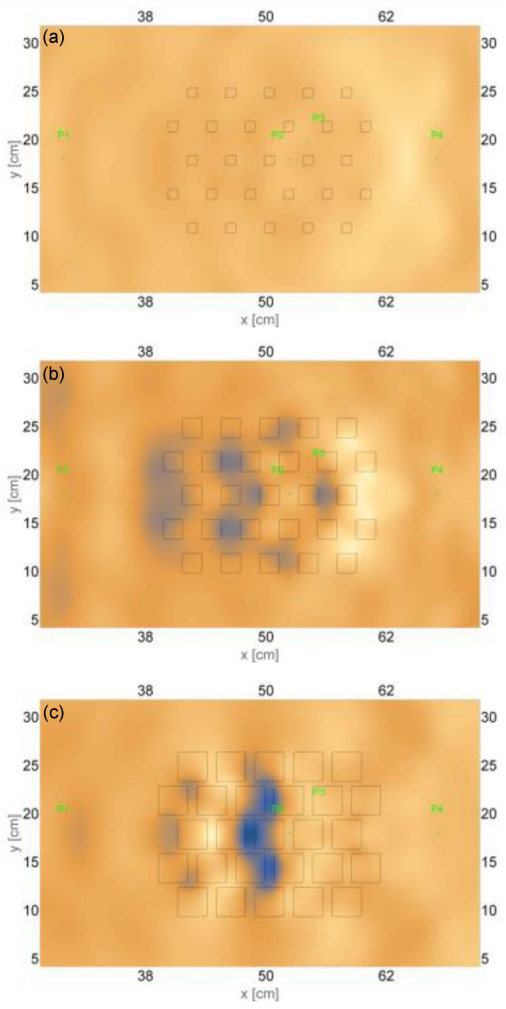

Fig. 2. Pressure distribution after 5000 time steps for fill factors: (a) 7%, (b) 29%, and (c) 65%.

TABLE I

Material parameters used in simulation [25–27].

Material	c [m/s]	ρ [kg/m^3]	$Z \times 10^3$ [kg/(s m^2)]
A (air)	331.45	1.29	428
B (PLA)	1633	6829	11 152

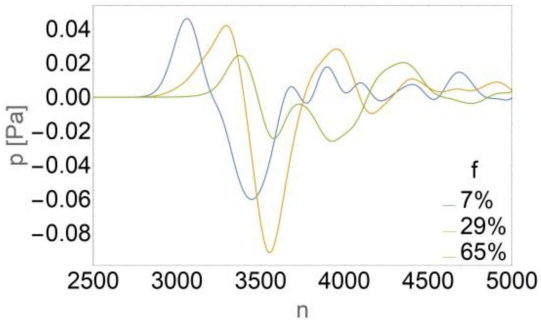

Fig. 3. Time series of pressure at point P4.

and

$$\frac{\partial v_y}{\partial t} = -\frac{1}{\rho}\frac{\partial p}{\partial y}, \tag{5}$$

which, after transformation to the formalism of the FDTD method, where $p|^n_{i,j}$ denotes the pressure value p at grid location ij and time instant n, takes the form

$$p|^{n+1}_{i,j} = p|^n_{i,j} - Z|_{i,j}\, c|_{i,j} \times \frac{\Delta t\left(v_x|^{n+\frac{1}{2}}_{i,j} - v_x|^{n+\frac{1}{2}}_{i-1,j} + v_y|^{n+\frac{1}{2}}_{i,j} - v_y|^{n+\frac{1}{2}}_{i,j-1}\right)}{\Delta z}, \tag{6}$$

$$v_x|^{n+\frac{1}{2}}_{i,j} = v_x|^{n-\frac{1}{2}}_{i,j} - \frac{\Delta t\left(p|^n_{i+1,j} - p|^n_{i,j}\right)}{\rho|_{i,j}\,\Delta z}, \tag{7}$$

$$v_y|^{n+\frac{1}{2}}_{i,j} = v_y|^{n-\frac{1}{2}}_{i,j} - \frac{\Delta t\left(p|^n_{i,j+1} - p|^n_{i,j}\right)}{\rho|_{i,j}\,\Delta z}. \tag{8}$$

Figure 1 shows the analyzed computational region surrounded by the boundary conditions of perfectly matched layers (PML) in order to suppress the wave propagating outside the simulation region. Point S is the source of the impulse described by the relation

$$p|^n_S = p|^n_S + \sin(3000\pi\, n\, \Delta t)\, \mathrm{e}^{-0.2\,((305-n)/50)^2}. \tag{9}$$

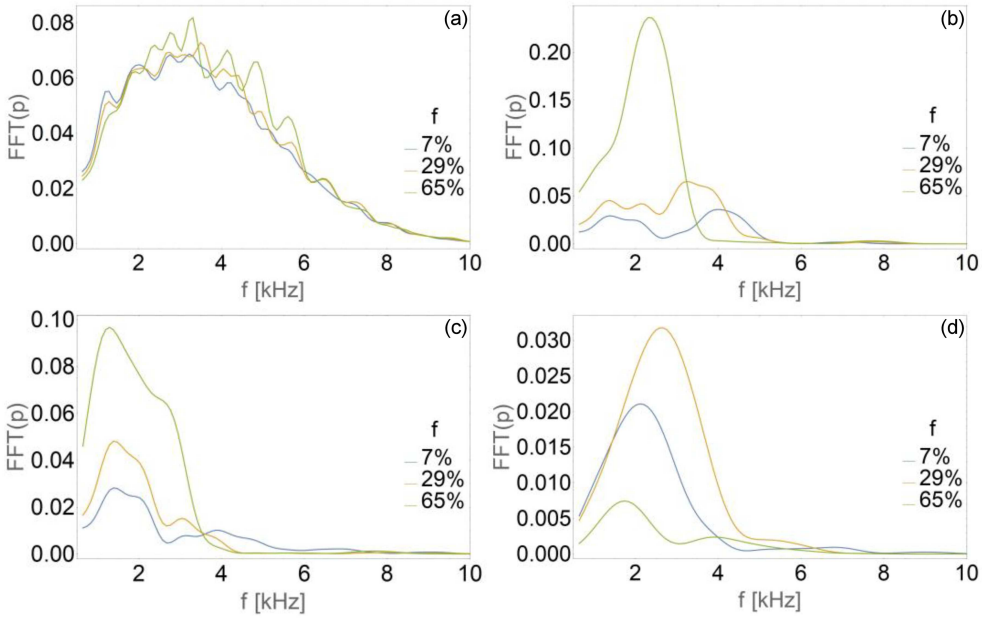

Fig. 4. Waveform spectra at the analyzed measurement points: (a) P1, (b) P2, (c) P3, and (d) P4.

In this work, a square grid with a spatial step of $\Delta z = 0.0025$ m was used. The time step was related to the spatial step of the Courant stability condition and amounted to $\Delta t = 5.435 \times 10^{-7}$. Figure 1 shows the measurement points from which the series of pressure changes in time were subjected to Fourier analysis. To smooth the spectrum, the Daniell window at $M = 6$ was used. At point P1, a wave propagating towards the structure and then reflected from it was analyzed. The nature of the wave transmitting through the structure was studied at point P4. Points P2 and P3 were chosen as characteristic points for studying the phenomenon of local resonances in the inter-meta-atomic space. The meta-atoms had a square cross-section with sides of 1 cm, 2 cm, and 3 cm, which for a hexagonal lattice with a lattice constant of 4 cm corresponded to fill factors f of 7%, 29%, and 65%, respectively. The meta-atom material was polylactic acid (PLA), which is often used for 3D printing. It was designated as material B, and its material parameters are presented in Table I (see also [25–27]). The wave propagation took place in air (material A).

Figure 2 shows the pressure distribution in the tested hexagonal phononic structure after 5000 time steps for the analyzed values of the fill factors.

The mechanical wave propagating in the structure with $f = 7\%$ (Fig. 2a) was not significantly disturbed by the presence of meta-atoms, and no local resonance areas were observed. In the second case ($f = 29\%$, Fig. 2b), local resonance areas of smaller amplitude were created due to the distribution of the wave energy over a larger area. At a fill factor of 65% (Fig. 2c), local resonance areas of higher intensity were created, which was also associated with a greater delay in wave propagation through the structure than in the case of 29% (Fig. 3).

Figure 4 shows the spectra of mechanical waves in the analyzed measurement points after 5000 time steps. As can be seen, the spectrum of the wave reflected from the structure (Fig. 4a) does not differ significantly for the tested values of the fill factor. In Fig. 4b and 4c, it can be seen that with the increase in the fill factor value, the intensity of the mechanical wave in the local resonance areas occurring in the inter-meta-atomic zones increases. The highest wave transmission was observed for the fill factor of 29% (Fig. 4d), and the lowest for the value of 65%. For each of the analyzed structures, the transmission above 5 kHz was significantly reduced, although for the structure with $f = 65\%$, the waves were already attenuated at 3 kHz.

3. Conclusions

The paper analyses the propagation of a mechanical wave in phononic finite hexagonal structures with different values of the fill factor.

The occurrence of local resonance areas was observed for values of the fill factor above 29%, which affected the slowdown of the mechanical wave inside the phononic structure, and with the increase in the fill factor, the intensity of the wave in these areas also increased.

In addition, the analyzed structure filtered the mechanical wave by passing part of the wave energy with a frequency of up to 4 kHz, and, in the case of a fill factor of 65%, up to 3 kHz.

References

[1] H. Zhang, B. Liu, X. Zhang, Q. Wu, X. Wang, *Phys. Lett. A* **383**, 2797 (2019).

[2] H. Guo, X. Yang, Y. Zhu, *Comput. Methods Appl. Mech. Eng.* **380**, 113743 (2021).

[3] M.V. Golub, O.V. Doroshenko, S.I. Fomenko, Y. Wang, C. Zhang, *Int. J. Solids Struct.* **212**, 1 (2021).

[4] M. Sigalas, E. N. Economou, *Solid State Commun.* **86**, 141 (1993).

[5] M.S. Kushwaha, P. Halevi, G. Martínez, L. Dobrzynski, B. Djafari-Rouhani, *Phys. Rev. B* **49**, 2313 (1994).

[6] J.A. Kulpe, K.G. Sabra, M.J. Leamy, *J. Acoust. Soc. Am.* **137**, 3299 (2015).

[7] L. Luschi, F. Pieri, *Proc. Eng.* **47**, 1101 (2012).

[8] A. Khelif, B. Aoubiza, S. Mohammadi, A. Adibi, V. Laude, *Phys. Rev. E* **74**, 046610 (2006).

[9] X. Pu, Z. Shi, *Soil. Dyn. Earthq. Eng.* **121**, 75 (2019).

[10] C. Zhao, J. Zheng, T. Sang, L. Wang, Q. Yi, P. Wang, *Construct. Build. Mater.* **283**, 122802 (2021).

[11] C. Qiu, Z. Liu, J. Mei, M. Ke, *Solid State Commun.* **134**, 765 (2005).

[12] J. Mei, Z. Liu, J. Shi, D. Tian, *Phys. Rev. B* **67**, 245107 (2003).

[13] J.-F. Lu, J. Cheng, Q.-S. Feng, *Eur. J. Mech. A Solids* **91**, 104426 (2022).

[14] S.-H. Jo, H. Yoon, Y.C. Shin, B.D. Youn, *Int. J. Mech. Sci.* **193**, 106160 (2021).

[15] S. Garus, W. Sochacki, *Wave Motion* **98**, 102645 (2020).

[16] Y. Jin, X.-Y. Jia, Q.-Q. Wu, X. He, G.-C. Yu, L.-Z. Wu, B. Luo, *J. Sound Vib.* **521**, 116721 (2022).

[17] A. Mehaney, A.M. Ahmed, F. Segovia-Chaves, H.A. Elsayed, *Optik* **244**, 167546 (2021).

[18] F.-L. Li, C. Zhang, Y.-S. Wang, *Eng. Anal. Bound. Elem.* **131**, 240 (2021).

[19] Q. Wei, X. Ma, J. Xiang, *Eng. Anal. Bound. Elem.* **134**, 1 (2022).

[20] H. Zheng, C. Zhou, D.-J. Yan, Y.-S. Wang, C. Zhang, *J. Comput. Phys.* **408**, 109268 (2020).

[21] A. Kupczyk, J. Świerczek, M. Hasiak, K. Prusik, J. Zbroszczyk, P. Gębara, *J. Alloys Compd.* **735**, 253 (2018).

[22] M.M. Sigalas, N. García, *J. Appl. Phys.* **87**, 3122 (2000).

[23] J.-H. Sun, T.-T. Wu, *Phys. Rev. B* **76**, 104304 (2007).

[24] N. Aravantinos-Zafiris, F. Lucklum, M.M. Sigalas, *Ultrasonics* **110**, 106265 (2021).

[25] D. Tarrazó-Serrano, S. Castiñeira-Ibáñez, E. Sánchez-Aparisi, A. Uris, C. Rubio, *Appl. Sci.* **8**, 2634 (2018).

[26] S. Yang, W.-D. Yu, N. Pan, *Phys. B Condens. Matter* **406**, 963 (2011).

[27] Y. Wang, W. Song, E. Sun, R. Zhang, W. Cao, *Phys. E Low-Dimen. Syst. Nanostruct.* **60**, 37 (2014).